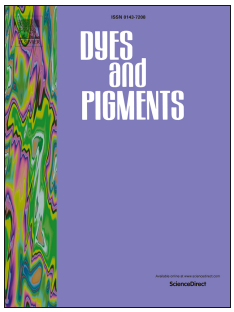

Effect of ionizing radiation on the colorimetric properties of PVA-GTA Xylenol Orange Fricke gel dosimeters

Salvatore Gallo, Stefania Pasquale, Cristina Lenardi, Ivan Veronese, Anna Maria Gueli

PII: S0143-7208(21)00009-7

DOI: https://doi.org/10.1016/j.dyepig.2021.109141

Reference: DYPI 109141

To appear in: *Dyes and Pigments*

Received Date: 14 September 2020

Revised Date: 5 January 2021

Accepted Date: 5 January 2021

Please cite this article as: Gallo S, Pasquale S, Lenardi C, Veronese I, Gueli AM, Effect of ionizing radiation on the colorimetric properties of PVA-GTA Xylenol Orange Fricke gel dosimeters, *Dyes and Pigments*, https://doi.org/10.1016/j.dyepig.2021.109141.

CRediT author statement

Title: Effect of ionizing radiation on the colorimetric properties of PVA-GTA Xylenol Orange Fricke gel dosimeters

Salvatore Gallo: Conceptualization, Supervision, Formal analysis, Data Curation, Writing - Original Draft. **Stefania Pasquale:** Methodology, Formal analysis, Data Curation, Writing - Original Draft. **Cristina Lenardi:** Methodology, Resources, Writing - review & editing. **Ivan Veronese**: Methodology, Supervision, Writing - review & editing. **Anna Maria Gueli:** Conceptualization, Resources, Supervision, Writing - review & editing.

Effect of ionizing radiation on the colorimetric properties of PVA-GTA Xylenol Orange Fricke gel dosimeters

Salvatore Gallo[1], Stefania Pasquale[2,*], Cristina Lenardi[1,3], Ivan Veronese[1], Anna Maria Gueli[2]

(1) Dipartimento di Fisica "Aldo Pontremoli" – Università degli Studi di Milano, Milano (Italy) and Istituto Nazionale di Fisica Nucleare (INFN) – Sezione di Milano, Milano (Italy)
(2) Dipartimento di Fisica e Astronomia "Ettore Majorana" – Università degli Studi di Catania, Catania (Italy) and Istituto Nazionale di Fisica Nucleare (INFN) – Sezione di Catania, Catania (Italy)
(3) Interdisciplinary Centre for Nanostructured Materials and Interfaces (CIMaINa), Milano (Italy)

Corresponding author:

**Pasquale Stefania*
Università degli Studi di Catania and INFN sez. CT
Via Santa Sofia 65 Catania, I-95123 Italy
e-mail: stefania.pasquale@ct.infn.it

Abstract

Fricke gel dosimeters were prepared using a matrix based on poly(vinyl-alcohol) chemical cross-linked with glutaraldehyde and loaded with Xylenol Orange. The samples were irradiated with gamma rays to doses in the range of 5-30 Gy and the consequent color changes were investigated by using spectrophotometry and colorimetry techniques.

Starting from the measurement of the transmittance spectra, an analysis of the color of the dosimeters was carried out considering the CIELAB color space. It allowed to highlight correlations between the color coordinates and the dose. Furthermore, the auto-oxidation processes occurring in the samples was studied by colorimetric measurements on both un-irradiated and irradiated samples at different times, up to two-week post-irradiation. The results showed no significant differences in the oxidation effect on the dosimeters, at least in the investigated dose interval.

The study suggested that colorimetric analysis, combined with the spectrophotometric one, can be a useful tool for characterizing the samples in view of a standardization of Fricke gel dosimetry.

Keywords: Gel dosimeters, Radio-chromic gels, Poly (vinyl alcohol), Xylenol Orange, Colorimetry.

1. Introduction

Radiation dosimetry refers to the measurement and/or calculation of the dose absorbed by an object as consequence of the interaction of ionizing radiation. Dosimetry is essential in many applications like radiotherapy, food irradiation and radiation sterilization. The dose, measured in gray (Gy=J/kg), consists in the energy deposited, by ionizing radiation, per unit mass of matter being irradiated. Over the years, the physicists have developed several systems to measure the radiation dose or, more in general, to characterize the quality of an ionizing radiation field [1]. These include ionization chambers, radiographic and radiochromic film, semiconductor detectors, thermoluminescence and optically stimulated luminescence, scintillation dosimeters and electron spin resonance dosimeters [1-7]. However, current dosimeters are only able to measure the dose in a limited volume (1D dosimeters) or in a plane (2D dosimeters) and thus they cannot provide a dose distribution over larger three dimensional (3D) volumes [8]. Recording the distribution of the dose in three dimensions is characteristic of gel dosimetry [9] and in particular of Fricke Gel (FG) [10].

In FG dosimetry, ferrous ions (Fe^{2+}) are dissolved in an acidic medium and the interaction of ionizing radiation with the gel causes water radiolysis, followed by and a series of chemical reactions leading to the conversion of Fe^{2+} to ferric ions (Fe^{3+}). The final concentration of Fe^{3+} is proportional to the absorbed dose, up to saturation [11].

The presence of paramagnetic Fe^{3+} alters the proton relaxation times of water and these changes can be measured by means of Nuclear Magnetic Resonance (NMR) relaxometry [12] and Magnetic Resonance Imaging (MRI) [10,13]. Furthermore, the spatial distribution of Fe^{3+} can be used to produce a 3D dose map by optical imaging [14,15] if a suitable metallic ion indicator is added to the gel matrix [16-19].

The most used metallic-ion indicator is Xylenol Orange (XO) sodium salt. The Fe^{3+} binds to XO forming a colored complex (XO–Fe^{3+}) that can be detected by spectrophotometric techniques. Actually, this complex absorbs light in the green-yellow spectral region 500-600 nm, making the irradiated Fricke gel dosimeters easily recognizable with the naked eye [20-22]. Indeed, their color changes from yellow to purple with increasing the absorbed dose.

Several papers available in the literature focused on the effects produced by the ionizing radiation on the optical and structural properties for different materials. In many cases, the color changes induced by radiation can be correlated with the absorbed. [23-37].

In this study the effect of gamma irradiation on the colorimetric properties of the Fricke gels loaded with Xylenol Orange was investigated and correlations between absorbed dose and color changes were discussed. The optical characterization of the irradiated gels was performed (i) by spectrophotometry for assessing the transmittance properties, and (ii) by the colorimetry for the color specification using the system codified by the *Commission Internationale d'Eclairage* (CIE).

It is worth noting that spectrophotometry allows measuring the intensity-energy relationship in selected regions of the electromagnetic spectrum. It analyzes the reflecting, absorbing or transmitting properties of samples without human interpretation and it can be indirectly linked to the colorimetric information using the

color matching functions and the spectral power distribution of the illuminant according to CIE standard rules [38].

The spectral transmittance information obtained by spectrophotometry was combined with colorimetry that performs a psychophysical analysis combining the physical stimulus resulting from the interaction of light with objects, with the response of the human visual system, which is based on the spectral sensitivities of the three photoreceptors of human eye, the tristimulus values.

In particular, after the assessment of the optical transmittance characteristics of the investigated Fricke gel dosimeters, we correlated their color with the absorbed dose and explored the color coordinate mostly influenced by the dose. Color measurements at different times post-irradiations were also performed. We chose the CIELAB 1976 color space that is one of the most used for communicating and expressing color in the research field considered. Furthermore, the CIELAB color space was designed to be perceptually uniform with respect to human color vision, which means that the same amount of numerical variation corresponds to approximately the same amount of change perceived visually [38].

We performed the experiments using dosimeters prepared with a gel matrix composed by synthetic hydrogels based on poly(vinyl-alcohol) (PVA) chemical cross-linked with glutaraldehyde (GTA) and loaded with XO. Such composition proved to be characterized by a diffusion rate of ferric ions significantly lower that what achievable with natural gel matrices like gelatin from porcine skin and agarose [39,40]. For this reason, the interest toward PVA-GTA Fricke gel dosimetry is gaining importance, as attested by the increasing literature about this topic [41-47]. The PVA-GTA Fricke gels have, in fact, sensitivities comparable to the conventional gel dosimeters and they are promising tools in X-ray external radiotherapy applications. It has been demonstrated that PVA-GTA Fricke gels are almost tissue equivalent over a very large photon energy range with independent dose rates and radiation energy [45].

2. Materials and Methods

2.1 Samples preparation

The PVA-GTA-FG dosimeters were prepared using ultrapure water (resistivity 18.2 MΩ·cm), obtained by a water purification system (Milli-Q® Direct, EMD Millipore, Germany), and using the following analytical grade compounds: 8.0 % w/w poly(vinyl alcohol) (PVA, Mowiol®18-88, Sigma Aldrich [48]), 0.5 mM ferrous ammonium sulfate hexahydrate (FAS, Carlo Erba); 0.165 mM Xylenol Orange tetra-sodium salt (XO, Riedel-de Haën), 21.2 mM of glutaraldehyde (GTA, Sigma Aldrich), and 25 mM of sulfuric acid (SA, Sigma Aldrich). The procedure for PVA-GTA Fricke gel dosimeters preparation, described in detail elsewhere [45], is here briefly summarized.

PVA solution was prepared by dissolving dry PVA in ultrapure water (80% of the total water volume) at 70 °C under magnetic stirring. After the complete dissolution, the PVA solution was left to cool down at room temperature (*i.e.* 18°C). Then, Fricke-XO solution was prepared by adding SA, FAS and XO in this order into ultrapure water (20% of the total water volume) with moderate stirring.

Finally, FG dosimeters were obtained by incorporating Fricke-XO solution into the PVA solution (with a rate of about 10 ml/min) and subsequently by adding the GTA under a slow magnetic stirring of 50 revolutions per minute (rpm).

The final solution was poured into UV-Vis standard cuvettes (10 mm optical path length) closed with cuvette-stoppers and sealed with Parafilm™. In addition, other FG dosimeters were obtained by pouring the solution into parallelepiped polyethylene-vessels (10 mm optical path length, 12 mL volume) and equipped with a stopper and sealed with Parafilm™. These samples were used for colorimetric investigations. After the complete gelation, all the Fricke gel dosimeters were stored in the dark at the controlled temperature of 6°C in order to minimize auto-oxidation phenomena [49]. The samples were brought back to room temperature 1 hour before the irradiations and optical measurements.

2.2 Samples irradiation

To assess the dose-response of the PVA-GTA Xylenol Orange Fricke gel dosimeters were uniformly irradiated, with an IBL 437C ^{137}Cs blood irradiator at the "Fondazione IRCCS Istituto Nazionale dei Tumori" of Milano (Italy) at room temperature ad using a dose rate of 11 cGy/s. [22]. The irradiations were performed the after their preparation.

The dose interval 5-30 Gy was selected for covering a range of clinical interest for conventional and stereotactic radiotherapy practices. For each dose value, three samples were irradiated. Figure 1 shows the picture of various Fricke gel dosimeters irradiated to different doses, together with an un-irradiated sample (0 Gy). The figure highlights that the color changes induced by gamma irradiation are visible with naked eye.

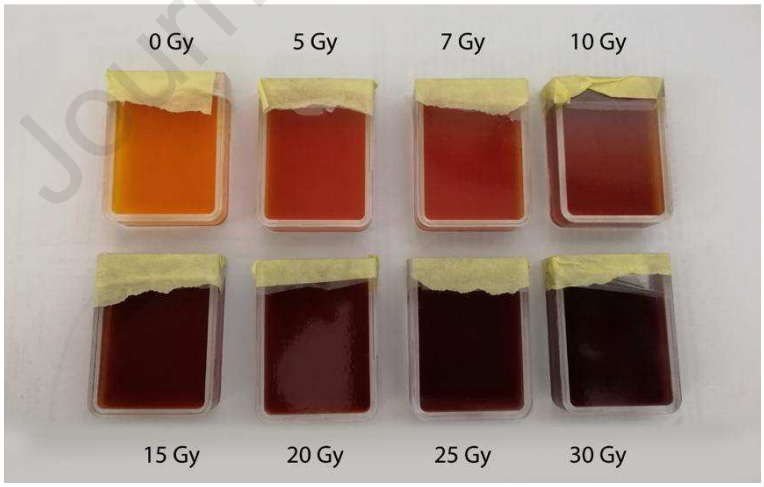

Figure 1- Picture of PVA-GTA-FG inside cuvettes for colorimetric measurements, irradiated at different doses in the interval 5-30 Gy, together with an un-irradiated sample (0 Gy). The delivered dose was reported near to the sample.

In the range of dose irradiation, the choice of the lower value is linked to the delivered dose uncertainty. Preliminary studies indeed have shown that time irradiation values lower than 30 seconds (corresponding to a dose of about 3 Gy) leads to an uncertainty greater to 10% of the dose value. For this reason, the experiments started from 5 Gy.

2.3 Optical Measurement

An UV-Vis spectrophotometer (Cary 100 UV-Vis, Agilent Technologies, Santa Clara, CA, USA) was employed for optical transmittance (T) measurements of the samples in the wavelength range of 380-780 nm with steps of 1 nm. Optical transmittance spectra were acquired using one cuvette filled with ultrapure water as a reference. In order to highlight optical changes due to the irradiation, the differences in optical transmittance Δ(T) between the irradiated samples and an un-irradiated one were considered. The measurements were performed approximately one-hour post-irradiation [40].

2.4 Color measurement

The measurements were performed using a Konica Minolta CR5 colorimeter with the transmission geometry known as "di:180°". This means that the sample receives the diffuse illumination and the total transmitted light, consisting of diffuse and directional components, was detected at 180°.

The transmittance measurements are carried out on gel samples contained in rectangular cells composed of glass for transmittance measurement with an optical path of 10 mm. For this experiment, the D65 illuminant and the CIE 1964 standard colorimetric observer were used. The standard CIE observer for 10° visual field was employed because it is mainly used in industrial colorimetry and the daylight illuminants simulates the sunlight environmental conditions. The selected illuminant, in fact, is denoted by the D that stands for daylight and the number 65 specifying the correlated color temperature expressed in kelvin and divided by 100. The scale adjustment, fundamental in colorimetry practice [50], was performed by the black (0%) and the white calibration (100%) references with which the instrument is equipped. The color measurements were carried out at different times on the same set of irradiated gels in order to check any changes due to the auto-oxidation process. With this purpose, we named time 0 (t=0) the first colorimetric measurement carried out one-day post-irradiation, and time 1 and 2 the acquisitions made after one and two weeks, respectively.

Starting from the CIE tristimulus values XYZ, we discussed the colorimetric results considering the CIELAB color space defined by CIE in 1976 [38], as done in previous studies conducted in the same field [23-29]. The XYZ values, for a transmitting sample, were calculated considering the product of the spectral power distribution of illuminant, the spectral transmittance of the FG and the color matching functions of the observer at each wavelength of the visible spectrum as given by the following equations (Equations 1) [51,52].

$$X = k\int_{380}^{780} P(\lambda)\bar{x}(\lambda)T(\lambda)d\lambda$$
$$Y = k\int_{380}^{780} P(\lambda)\bar{y}(\lambda)T(\lambda)d\lambda$$
$$Z = k\int_{380}^{780} P(\lambda)\bar{z}(\lambda)T(\lambda)d\lambda \qquad \text{(Eq.1)}$$

where $P(\lambda)$ is the relative spectral power of a CIE standard light source at the wavelength λ, $T(\lambda)$ is the transmittance of the sample at the wavelength λ, and $\bar{x}(\lambda)$,$y(\lambda)$ and $\bar{z}(\lambda)$ are the CIE color matching

functions for the standard observer at the wavelength λ. The *k* factor normalizes the tristimulus value so that Y is equal to 100 for a perfect white diffuser [30]. Figure 2 shows, in the visible range (380-780 nm), the Color Matching Functions (CMF) $\bar{x}(\lambda)$,$y(\lambda)$ and $\bar{z}(\lambda)$ for the 10° standard observer and the spectral power distribution CIE illuminant D65 chosen in this experimental set-up [38].

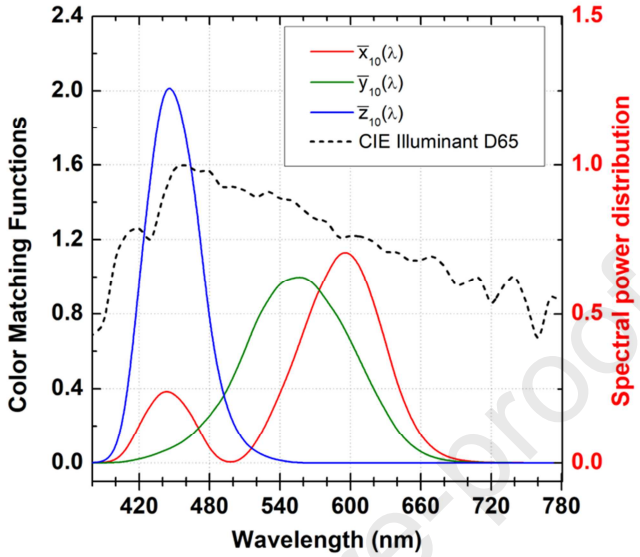

Figure 2 – The CIE Color Matching Functions $\bar{x}(\lambda)$, $y(\lambda)$ and $\bar{z}(\lambda)$ for the 10° standard observer (primary scale in black) and the spectral power distribution CIE illuminant D65 (secondary scale in red) are plotted in the 380-780 nm range with solid and dashed lines, respectively [51-52].

One of the main drawback of the tristimulus color space is the lack of perceptually uniformity, as pointed out in the "Supplementary Materials" and in the Figure S1a. For this reason, we used the CIELAB color space that better approximates human vision describing all the color visible to the human eye [45]. The CIELAB coordinates were calculated from the tristimulus values (Eq. 1) according to the following equations (Equations 2) [51]:

$$L^* = 116f\left(\frac{Y}{Y_n}\right)\text{-}16$$
$$a^* = 500\left[f\left(\frac{X}{X_n}\right) - f\left(\frac{Y}{Y_n}\right)\right]$$
$$b^* = 200\left[f\left(\frac{Y}{Y_n}\right) - f\left(\frac{Z}{Z_n}\right)\right] \qquad \text{(Eq.2)}$$

where $f(s)=s^{1/3}$ for $s > 0.008856$ and $f(s)=7.787s+16/116$ for $s \leq 0.008856$ and *X*, *Y* and *Z* are the tristimulus values. In Eq. 2 the same values with the subscript *n* refer to the tristimulus values of the perfect diffuser for the given illuminant and standard observer [51]. In CIELAB color space, the color is mapped onto a three-dimensional space in which L* coordinate indicates the darkness and lightness axis and the coordinates a∗ and b∗ are associated to red (positive values) and green (negative values), and yellow (positive values) and blue (negative values), respectively. In the CIELAB color space–the same amount of numerical variation corresponds to approximately the same amount of change perceived visually [38]. More details on color spaces are given in Figure S1b of the "Supplementary Materials".

The CIELAB color difference between two colors is represented by the Euclidean distance ΔE^*_{ab}, expresses by the equation 3a [51]:

$$\Delta E^*_{ab} = [(L^*_2 - L^*_1)^2 + (a^*_2 - a^*_1)^2 + (b^*_2 - b^*_1)^2]^{\frac{1}{2}} \quad \text{(Eq.3a)}$$

In our case, the subscripts 1 and 2 refer to the un-irradiated and to the irradiated samples, respectively. Equation 3a, with the obviously meaning of the symbols, can be rewritten as:

$$\Delta E^*_{ab} = [(\Delta L)^2 + (\Delta a^*)^2 + (\Delta b^*)^2]^{\frac{1}{2}} \quad \text{(Eq.3b)}$$

3. Results and Discussion

Figure 3 shows some examples of optical transmittance spectra of FG dosimeters irradiated to different doses (panel a), together with the spectra of the optical transmittance variation Δ(T) as effect of the gamma irradiation (panel b). It can be observed that the transmittance decreases with increasing the radiation dose in the wavelength region 500 nm - 600 nm (green region). In fact, it is known that the irradiated FG dosimeters loaded with XO are characterized by a broad optical absorption peak around 585 nm [21]. Additional details about the absorbance spectra of these dosimeters and their relationship with the absorbed dose are given in the "Supplementary Materials" (Figure S3). The transmittance spectra have been used to highlight the relationship with the colorimetric analysis performed by colorimeter.

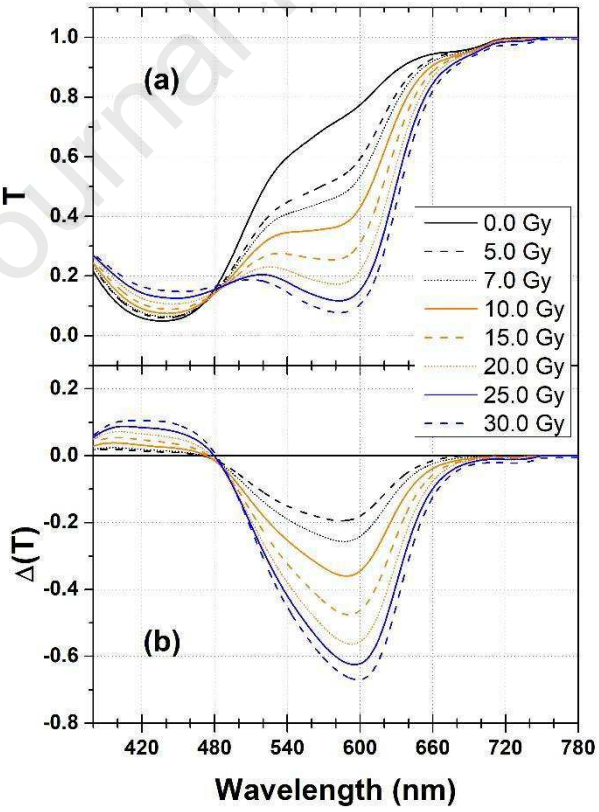

Figure 3 – Optical transmittance spectra of PVA-GTA Fricke gels irradiated to different doses (panel a), and corresponding optical transmittance variation Δ(T) spectra (panel b).

Starting from the transmittance spectra and considering the approach described in Section 2.4, the CIE tristimulus values XYZ of the investigated FG dosimeters were derived and their spectra are shown in Figures 4-6 in the interval of the visible electromagnetic spectrum (380-780 nm) according to CIE [51]. From the curves' trends of XYZ we can gather some color information about what happens in the gel with the gamma irradiation. It can be observed that Z increases with increasing the radiation dose. It means that the blue color perception of the samples is progressively enhanced with increasing the dose absorbed by the Fricke gel dosimeters. By contrast, X and Y decrease with increasing dose, indicating a progressive reduction of the yellow-orange (450-650 nm) perception of the irradiated samples. Furthermore, X and Y spectra show at least two peaks in the region between 500-650 nm, deriving from the transmittance curves. They are related to the chemical reactions occurring between radio-induced ferric ions and XO as effect of the gamma irradiation which produce different types of complexes [54]. For more clarity, the trends of X, Y and Z coordinates versus dose are reported in the "Supplementary Material" in Figure S2.

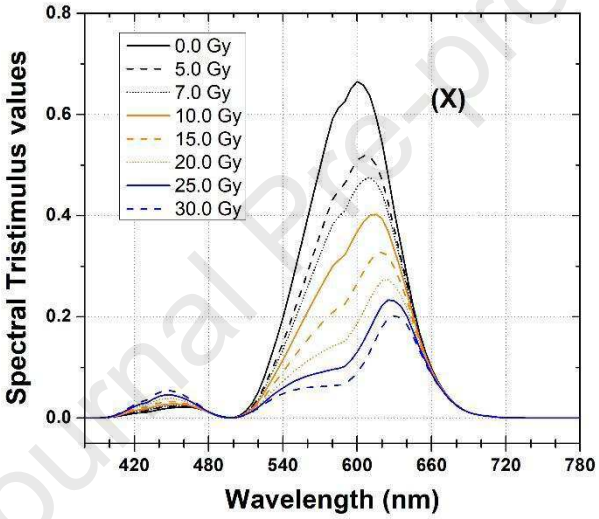

Figure 4 – X values in the visible range of the electromagnetic spectrum of Fricke gel samples irradiated to different doses.

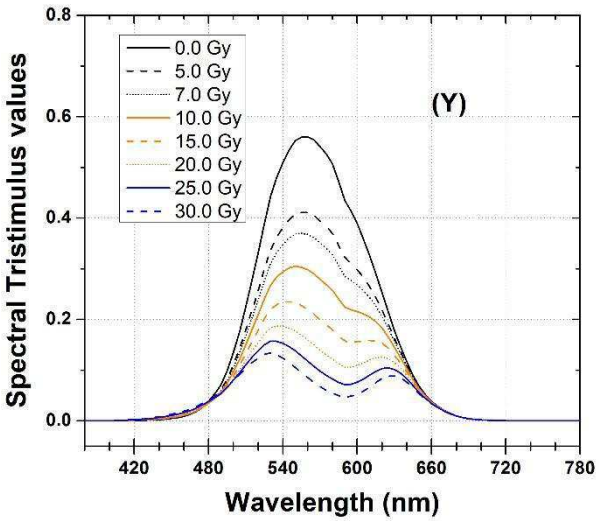

Figure 5 – Y values in the visible range of the electromagnetic spectrum of Fricke gel samples irradiated to different doses.

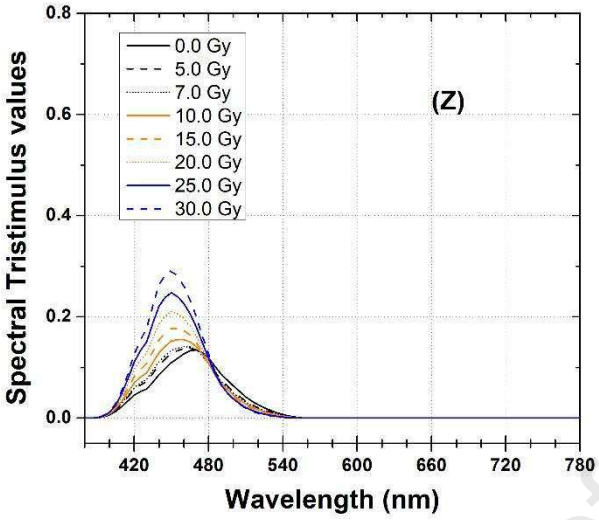

Figure 6 – Z values in the visible range of the electromagnetic spectrum of Fricke gel samples irradiated to different doses

As explained in Section 2.4, in addition to the XYZ values, the color coordinates in the CIELAB color space were derived to better investigate and quantify the color differences of the irradiated samples. The color differences ΔL*, Δa*, Δb* and ΔE^*_{ab}, calculated using Eq. 2 and 3, are reported in Table 1. Using these values it is possible to detect color variations that are not visible with the naked eye, and to establish thresholds revealing significant color changes. In fact, unlike the human eye perception, in the CIELAB color space it is possible to define tolerance values and range for acceptability, useful for various applications. Tolerance values should correlate to the human eyes so that color is both visually and numerically acceptable. This ensures, for instance, consistency from one batch of material to the next one. It is worth noting that only trained observers can notice color differences characterized by ΔE*ab ranging from 1 to 2. By contrast, ΔE*ab values greater than 5 can be easily noticed by all observers [55]. In the case of the irradiated Fricke gel dosimeters, considering the dose range selected for the experiments, significantly high ΔE*ab values were obtained.

Among the various color differences shown in Table 1, ΔL*, Δa* and Δb* are of particular interest since they are related to changes in color brightness and in terms of red (positive) -green (negative) and yellow (positive) -blue (negative) shifts, respectively.

Table 1 – ΔL*, Δa*, Δb*, ΔE^*_{ab} values, obtained using an un-irradiated gel as reference, and the related uncertainties for each irradiation dose (Gy) are listed. The uncertainties were calculated by the propagation of uncertainties.

Dose (Gy)	**ΔL***	**Δa***	**Δb***	ΔE^*_{ab}
5	-16.8 ±0.1	5.7 ±0.1	-25.5 ±0.2	31.1 ±0.2
7	-21.6 ±0.1	6.7 ±0.1	-32.7 ±0.2	39.7 ±0.2
10	-29.3 ±0.1	7.9 ±0.1	-46.0 ±0.2	55.1 ±0.2
15	-38.2 ±0.1	8.8 ±0.1	-61.9 ±0.2	73.3 ±0.2
20	-44.5 ±0.2	9.0 ±0.1	-74.3 ±0.2	87.1 ±0.3
25	-48.7 ±0.2	8.7 ±0.1	-83.8 ±0.2	97.3 ±0.2
30	-51.8 ±0.1	8.2 ±0.1	-91.8 ±0.2	105.8 ±0.2

ΔL* values are negative and decrease dose from -16.8 (5 Gy) to -51.8 (30 Gy), indicating that the gel samples become darker with increasing the absorbed dose. Δa* are positive, characterized by very small values compared to the other color differences, and without any monotonic trend with the radiation dose. Finally, considering the Δb* negative values, significant blue-shifts were obtained, as expected. In fact, the color of the Fricke gel dosimeters changes, when observed with naked eye, from orange to purple, with increasing the radiation dose.

The plots of the L*, a* and b* color coordinates versus radiation dose are shown in Figure 7. In this figure, the dash blue line is a guide for the eye obtained using a basis spline function. By contrast, the solid red lines are fitted curves to the experimental data over the whole dose interval.

Figure 7a shows the decrescent exponential trend that described the behavior of L* coordinate with the dose. In the same Figure, the a* and b* coordinates (Figure 7b-c) are shown. As highlighted in Figure 7b the a* coordinate presents two types of responses. Until 5 Gy the samples are subjected to a red-shift, quantified in Table 1 by Δa*=5.7. Then, the behavior seems to be monotone and, in the higher doses region, it becomes slightly decreasing.

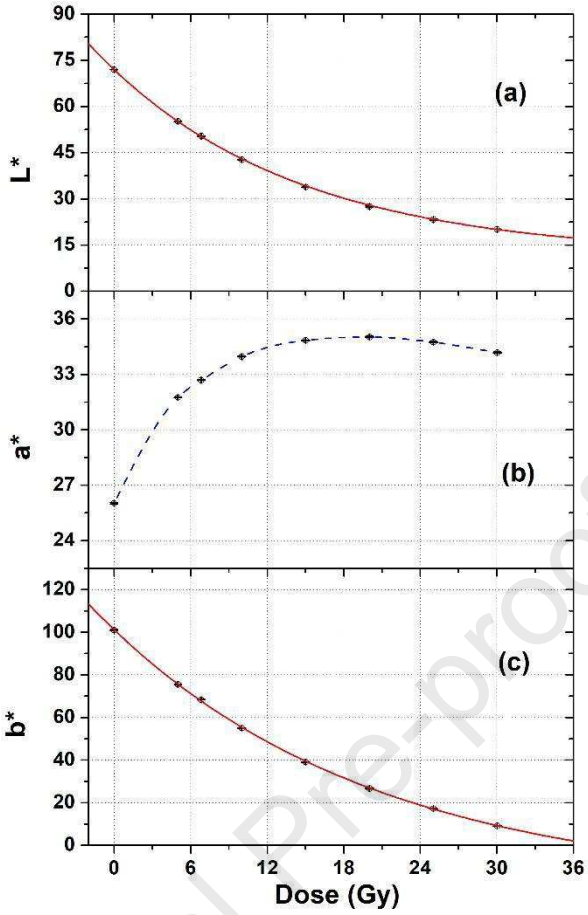

Figure 7 - (a) L*, (b) a* and (c) b* color coordinates versus radiation dose. The dash blue line is a guide for the eye obtained using a basis spline function. The solid red lines are fitted curves to the experimental data over the whole dose interval.

In detail, the exponential function:

$$CC = A * exp^{(-\frac{Dose}{B})} + C \qquad \text{(Eq.4)}$$

was fitted to the experimental data related to the L* and b* coordinates. In Equation 4, CC are the color coordinates (L* and b*) and A, B, C the fit parameters (A is a scaling factor, B is the parameter related to exponential decay and C is the offset). The values of the fit parameters together with the R^2 index are shown in Table 2.

Table 2 – The exponential fit parameters of the L* and b* coordinates obtained by color measurements.

CC	A	B	C	R^2
L*	60.3±0.4	15.1±0.3	11.8±0.5	0.9998
b*	120.9±1.5	20.9±0.5	-19.7±1.6	0.9998

In order to investigate and quantify color changes due to the auto-oxidation process occurring in the Fricke gel dosimeters, the b* coordinate was evaluated at different times post-irradiation, as explained in Section 2.4.

Figure 8a shows the trend of b* values vs dose obtained up to two weeks post-irradiation.

In the Figure the t=0 indicates the first colorimetric measurement after irradiation and t=1 and t=2 the acquisitions made after one and two weeks later respectively.

Each point in Figure 8b is the mean value of three measurements performed on different samples. The error bars, corresponding to one standard are included in the size of the symbols.

Using the exponential fit parameters of Table 2 related the b* coordinate obtained at t=0, the reconstructed dose values achievable at different times post-irradiation were calculated using the following Equation 5:

$$Reconstructed_{DOSE} = -B * ln\left(\frac{b^* - C}{A}\right) \qquad \text{(Eq.5)}$$

Where A, B and C are the fit parameters previously mentioned for Eq.4.

Figure 8b shows the reconstructed dose values *vs* the delivered dose. The errors bars in Figure 8b, corresponding to one standard deviation, were calculated by the propagation of uncertainties, considering the uncertainties of the fit parameters A, B and C and the uncertainty in the experimental measurement of b*.

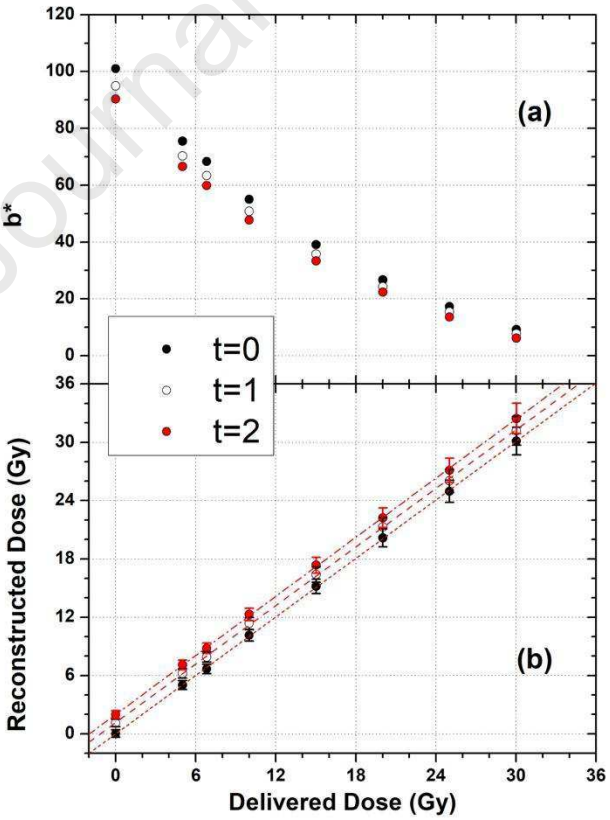

Figure 8 – (a) Trend of b* values vs dose measured at different times post-irradiation Each point is the mean value of three measurements performed on different samples. The error bars, corresponding to one standard deviation are smaller

than the dimensions of the symbols. (b) Reconstructed dose values vs the delivered dose at different times post-irradiation, together fitted straight-lines.

A linear function expressed by Equation 6:

$$Reconstructed_{DOSE} = m * Delivered_{DOSE} + q \qquad \text{(Eq.6)}$$

was fitted to the experimental data of Figure 8b. The values of the fit parameters related to the slope (m) and the intercept (q) of the fitted straight lines, are reported in Table 3, together with the R^2 indexes. It can be observed that the three fitted lines of Figure 8b differ only in the value of the intercept, that represent the dose related to the auto-oxidation of the gel samples.

For each dataset (i.e. for each post-irradiation time), the differences between the delivered doses and the reconstructed ones (ΔDose) were calculated. The corresponding mean values (mean ΔDose) and uncertainties (one standard deviations) are reported n in Table 3.

Table 3 – Values of the fit parameters indicating the slope (m) and the intercept (q) of the straight lines fitted to the data of the reconstructed dose vs delivered one. Values of R^2 and mean ΔDose are also reported. All the values are given with the associated uncertainties (Δm, Δq and σ).

Time (week)	**m±Δm**	**q±Δq**	**Mean ΔDose± σ**	**R^2**
0	1.003±0.005	0.00±0.05	0.07±0.09	0.9999
1	1.004±0.006	1.15±0.06	1.15±0.07	0.9998
2	1.008±0.005	2.05±0.05	2.11±0.06	0.9998

In Figure 9, the ΔDose values are plotted versus the delivered dose. The solid red lines and the dotted blue ones in Figure 9 represent the mean ΔDose values and the q values, respectively. No significant trends of the ΔDose values with increasing the delivered dose was observed, for all the three sets of measurements.

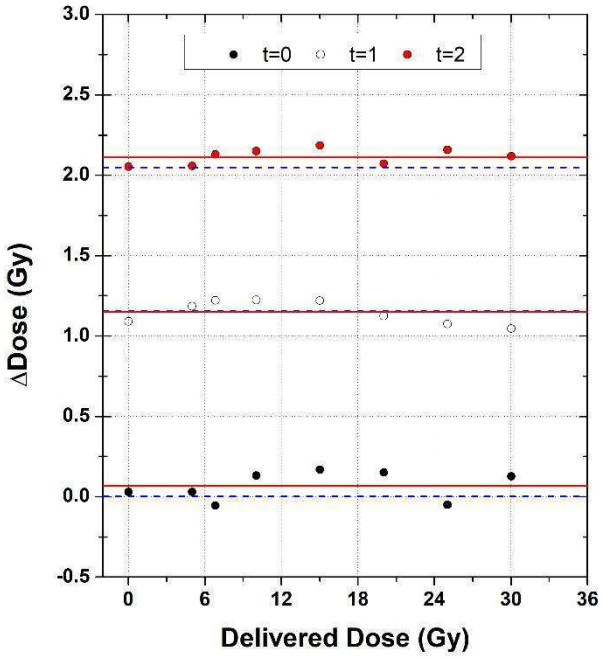

Figure 9 – Delta Dose (ΔDose) values vs the delivered dose for different post-irradiation times. The solid red lines and the dotted blue ones represent the mean ΔDose values and the q values reported in Table 3, respectively.

Using the unpaired t-test, confidence levels equal to 50%, 100% and 45%, between intercept parameters (q) and the mean ΔDose values were obtained, considering the data pairs at t=0, t=1 and t=2, respectively. It suggests that the oxidation process depends only on the time elapsed by the radiation and not on the dose, at least in the investigated interval. The same conclusion can be drawn by fitting the function of Eq. 4 to experimental data of Figure 8b and comparing the values of the fit parameter B. Values equal to 20.9±0.5, 20.2±0.4 and 20.4±0.4 were obtained for t=0, t=1 and t=2, respectively. Applying the unpaired t-test and considering the data pairs at t=0/t=1; t=0/t=2 and t=1/t=2, the confidence levels estimated are of 32%, 48% and 76%, respectively.

In fact, differences in the auto-oxidation of irradiated samples with the delivered dose could be expected only close to the saturation of the dosimeter's response when ferrous sulfate to oxidize is no more available (i.e. at doses higher than 30 Gy). It is worth noting that the same information would be attained by spectrophotometric analysis, as previously done with different Fricke gel matrices [11, 47].

4. Conclusions and Remarks

Fricke gels as dosimeters are well known tools in radiation dosimetry. As consequence of the interaction of ionizing radiation, ferrous ions (Fe^{2+}) are converted into ferric (Fe^{3+}) ions and, by adding Xylenol Orange sodium salt into the gel dosimeters, a colored complex (XO–Fe^{3+}) is formed. The study of the color of this complex and its variation with changing the radiation dose and the post-irradiation time was the object of this research.

Starting from the measurement of the transmittance spectra, an analysis of the color of PVA/GTA Fricke gels loaded with XO was carried out considering the CIELAB color space. The calculation of ΔL*, Δa*, Δb* allowed quantifying the color changes and to study possible correlation between the color coordinates and the dose. Exponential decreases of L* and b* with increasing the radiation dose were observed, attesting the effect of ionizing radiation to darken the samples and to change their color from orange to violet. By contrast, no significant correlation of the a* coordinate with the dose was observed.

The auto-oxidation processes of the samples were studied by assessing the b* values of both un-irradiated and irradiated samples at different times, up to two-weeks post-irradiation.

The results showed no significant differences in the oxidation effect on the dosimeters, at least in the investigated dose interval.

The methodological approach used in this research article is turned out to be very useful because it allowed to match information coming from transmittance and colorimetric measurements. It must be pointed out that, despite the long and extensive research carried out on Fricke gel dosimeters in the recent decades, these tools still require further optimization and standardization of the production procedure. When used in the clinical practice for 3D dose reconstruction, MRI and optical tomography are the reference techniques. However, as far as the research and development phase is concerned, the results of this study suggest that colorimetry,

combined with the well-established spectrophotometry techniques, can be useful for characterizing Fricke gel samples. The relevance of such color changes and the further variations due to the interaction of ionizing radiation or auto-oxidation processes can be easily detected and quantified by colorimetry. Furthermore, because any variation in the receipt and/or in the chemical components used for Fricke gel preparation may induce color changes in the sample, the colorimetry may contribute to the standardization of the Fricke gel dosimetry. With this purpose, a new campaign of color measurements has scheduled using different chelators (such as Methylthymol blue) that have a characteristic peak of optical absorption differing from the XO.

Acknowledgments

The authors wish to thank Daniela Bettega and Paola Calzolari, for their useful comments and suggestions. The authors are also grateful to Emanuele Pignoli for the irradiation of the samples at the "Fondazione IRCCS Istituto Nazionale dei Tumori".

References

[1] Seco J, Clasie B and Partridge M. Review on the characteristics of radiation detectors for dosimetry and imaging. Physics in Medicine and Biology 2014; 59(20):303-347.

[2] Asero G, Greco C, Gueli AM, Raffaele L, Spampinato S. Evaluation of spatial resolution in image acquisition by optical flatbed scanners for radiochromic film dosimetry. Journal of Instrumentation 2016, 11:P03024.

[3] Gueli AM, Cavalli N, De Vincolis R, Raffaele L, Troja SO. Background fog subtraction methods in Gafchromic® dosimetry. Radiation Measurements 2015, 72:44-52.

[4] Veronese I, Chiodini N, Cialdi S, d'Ippolito E, Fasoli M, Gallo S, La Torre S, Mones E, Vedda A, Loi G. Real-time dosimetry with Yb-doped silica optical fibres. Physics in Medicine and Biology 2017, 62(10):4218-4236.

[5] Marrale M, Abbene L, d'Errico F, Gallo S, Longo A, Panzeca S, Tana L, Tranchina L and Principato F. Characterization of the ESR response of alanine dosimeters to low-energy Cu-target X-tube photons. Radiation Measurements 2017, 106:200-204.

[6] Gallo S, Iacoviello G, Bartolotta A, Dondi D, Panzeca S and Marrale M. ESR dosimeter material properties of phenols compound exposed to radiotherapeutic electron beams. Nuclear Inst. and Methods in Physics Research, B 2017, 407:110-117.

[7] Gallo S, Iacoviello G, Panzeca S, Veronese I, Bartolotta A, Dondi D, Gueli A M, Loi G, Longo A, Mones E, Marrale M. Response characterization of phenolic solid state pellets for ESR dosimetry with radiotherapeutic photon beams. Radiation and Environmental Biophysics, 2017, 56(4):471-480.

[8] Pasler M, Hernandez V, Jornet N, Clark, C. Review: Novel methodologies for dosimetry audits: Adapting to advanced radiotherapy techniques Physics and Imaging in Radiation Oncology, 2018, 5:76-84.

[9] Doran S, The history and principles of chemical dosimetry for 3-D radiation fields: Gels, polymers and plastics. Applied Radiation and Isotopes 2009, 67:393–398.

[10] Gore JC and Kang YS, Measurement of radiation dose distributions by nuclear magnetic resonance (NMR) imaging. Physics in Medicine and Biology 1984, 29(10):1189-1197.

[11] Davies J and Baldock C, Sensitivity and stability of the Fricke-gelatin-xylenol orange gel dosimeter. Radiation Physics and Chemistry 2008: 77(6) 690–696.

[12] Marrale M, Brai M, Gagliardo C, Gallo S, Longo A, Tranchina L, Abbate B, Collura G, Gallias K, Caputo V et al., Correlation between ferrous ammonium sulfate concentration, sensitivity and stability of Fricke gel dosimeters exposed to clinical X-ray beams. Nuclear Instruments and Methods in Physics Research Section B 2014, 335:54–60.

[13] MacDougall N D, Pitchford W G and Smith M A, A systematic review of the precision and accuracy of dose measurements in photon radiotherapy using polymer and Fricke MRI gel dosimetry. Physics in Medicine and Biology 2002, 47(20):R107-21.

[14] Olding T, Holmes O and Schreiner L, Cone beam optical computed tomography for gel dosimetry I: scanner characterization. Phys. Med. Biol. 2010, 55:2819–2840.

[15] Colnot J, Huet C, Gschwind R and Clairand I. Characterisation of two new radiochromic gel dosimeters TruView™ and ClearView™ in combination with the vista™ optical CT scanner: A feasibility study. Physica Medica 2018, 52:154–164.

[16] Alves A, de Almeida S, Sussuchi M, Lazzeri L, d'Errico F and de Souza S. Investigation of chelating agents/ligands for Fricke gel dosimeters. Radiation Physics and Chemistry 2018, 150:151-156.

[17] Eyadeh M, Rabaeh K, Hailat T and Aldweri F. Evaluation of ferrous Methylthymol blue gelatin gel dosimeters using nuclear magnetic resonance and optical techniques. Radiation Measurements 2018, 108:26-33.

[18] Eyadeh M, Rabaeh K, Hailat T, Al-Shorman M, Aldweri F, Kanan H and Awad S. Investigation of a novel chemically cross-linked fricke-Methylthymol bluesynthetic polymer gel dosimeter with glutaraldehyde cross-linker. Radiation Measurements 2018, 118:77–85.

[19] Coulaud J, Brumas V, Sharrock P and Fiallo M. 3D optical detection in radiodosimetry: EasyDosit hydrogel characterization. Spectrochimica Acta Part A: Molecular and Biomolecular Spectroscopy 2019, 220:117124.

[20] Soliman Y, El Gohary M, Gawad M, Amin E and Desouky O, Fricke gel dosimeter as a tool in quality assurance of the radiotherapy treatment plans. Applied Radiation and Isotopes 2017, 120:126-132.

[21] Gambarini G, Veronese I, Bettinelli L, Felisi M, Gargano M, Ludwig L, Lenardi C, Carrara M, Collura G, Gallo S, et al. Study of optical absorbance and MR relaxation of Fricke xylenol orange gel dosimeters. Radiation Measurements 2017, 106:622-627.

[22] Gallo S, Cremonesi L, Gambarini G, Ianni L, Lenardi C, Argentiere S, Bettega D, Gargano M, Ludwig N and Veronese I. Study of the effect of laponite on Fricke xylenol orange gel dosimeter by optical techniques. Sensors and Actuators B: Chemical 2018, 272C:618-625.

[23] Oberoi P, Chandan F, Chandra M, Prakash M. Comparative study of two azo dyes using Triphenyl-Tetrazolium Chloride (TTC) on gamma irradiation induced film dosimeter. Nuclear Instruments and Methods in Physics Research Section B 2020, 466:82-89.

[24] Kozicki M, Sąsiadek E, Kadlubowski S, Dudek M, Maras P, Nosal A, Gazicki-Lipman M. Flat foils as UV and ionising radiation dosimeters. Journal of Photochemistry and Photobiology A: Chemistry 2018, 351:179–196.

[25] Nouh S A, Abutalib M M. A comparative study of the effect of gamma and electron beam irradiation on the optical and structural properties of polyurethane. Radiation Effects & Defects in Solids 2011, 166(3):165-177.

[26] Nouh S A, R Bahareth R A. Color changes in some irradiated polymers. Radiation Effects & Defects in Solids 2012, 167(10):766-773.

[27] Nouh S A, Bahareth R A. Effect of electron beam irradiation on the structural, thermal and optical properties of poly(vinyl alcohol) thin film. Radiation Effects & Defects in Solids 2013, 168(4):273-285.

[28] Raouafi A, Daoudi M, Jouini K, Charradi K, Hamzaoui AH, Blaise P, Farah K, Hosni F. Effect of gamma irradiation on the color, structure and morphology of nickel-doped polyvinyl alcohol films: alternative use as dosimeter or irradiation indicator. Nucl Instrum Methods Phys Res, Sect B 2018, 425:4–10.

[29] Hosni F, Farah K, Kaouach H, Louati A, Chtourou R, Hamzaoui AH. Effect of gamma-irradiation on the colorimetric properties of epoxy-resin films: potential use in dosimetric application. Nucl Instrum Methods Phys Res, Sect B 2013, 311:1–4.

[30] Said HM, Ali ZI, Ali HE. Physical Properties of Electron Beam Irradiated Poly(vinyl butyral) Composites with Carbamate, Imidazole, and Tetrazolium Dye. Journal of Applied Polymer Science 2006, 101:4358–4365.

[31] Kozicki M, Sąsiadek E, Karbownik I, Maniukiewicz W. Doped polyacrylonitrile fibres as UV radiation sensors Sensors and Actuators B 2015, 213:234–243.

[32] Ioan MR. An innovative idea for developing a new gamma-ray dosimetry system based on optical colorimetry techniques. Nuclear Engineering and Technology 2018, 50(3):519-525.

[33] Guesmi S, Raouafi A, Amri I, Hamzaoui AH, Boulila A, Hosni F, Sghaier H. Polyphenolic extracts from the xerophyte Rhamnus lycioides as a radiation biodosimeter. Environ Sci Pollut Res 2018, 27:5661–5669.

[34] Magida M, Abou El Fadl A, Nouh SA. Modifications induced in natural rubber due to vinylacetate versatic ester copolymer blend concentration and gamma radiation. Polymer Bulletin 2020, 77:6319–6332.

[35] Elhalawany N, Wassel AR, Abdelhamid AE, Elfadl AA, Nouh S. Novel hyper branched polyaniline nanocomposites for gamma radiation dosimetry. Journal of Materials Science: Materials in Electronics 2020, 31:5914–5925.

[36] Nouh SA, Benthami K, Samy RM, El-Hagg AA. Effect of gamma radiation on the structure and optical properties of polycarbonate-polybutylene terephthalate/silver nanocomposite films. Chemical Physics Letters 2020, 741:137123.

[37] Nouh SA, Benthami K, Abou El Fadl A, El-Shamy NT, Tommalieh MJ. Structural, thermal and optical characteristics of laser□exposed Pd/PVA nanocomposite. Polymer Bulletin 2020, 14.

[38] CIE 15:2004, Colorimetry, 3rd ed. Vienna: Commission Internationale de l'èclairage; 2004.

[39] Marrale M, Collura G, Gallo S, Nici S, Tranchina L, Abbate B, Marineo S, Caracappa S and d'Errico F. Analysis of spatial diffusion of ferric ions in PVA-GTA gel dosimeters analyzed via magnetic resonance imaging. Nuclear Instruments and Methods in Physics Research Section B 2017, 396:50–55.

[40] Marini A, Lazzeri L, Cascone M, Ciolini R, Tana L and d'Errico F. Fricke gel dosimeters with low-diffusion and high-sensitivity based on a chemically cross-linked PVA matrix. Radiation Measurements 2017, 106:618-621.

[41] Gallo S, Collura G, Longo A, Bartolotta A, Tranchina L, Iacoviello G, d'Errico F and Marrale M. Preliminary MR relaxometric analysis of Fricke-gel dosimeters produced with Poly-vinyl alcohol and glutaraldehyde. Nuclear Technology & Radiation Protection 2017, 32(3):242-249.

[42] Rabaeh K, Eyadeh M, Hailat T, Aldweri F, Alheet S and Eid R, Characterization of ferrous-methylthymol blue-polyvinyl alcohol gel dosimeters using nuclear magnetic resonance and optical techniques. Radiation Physics and Chemistry 2018, 148:25–32.

[43] Collura G, Gallo S, Tranchina L, Abbate B, Bartolotta A, d'Errico F and Marrale M, Analysis of response of PVA-GTA Fricke-gel dosimeters through clinical magnetic resonance imaging. Nuclear Instruments and Methods in Physics Research Section B 2018, 414:146-153.

[44] Eyadeh M, Rabaeh K, Aldweri F, Al-Shorman M, Alheet S, Awad S, Hailat T. Nuclear magnetic resonance analysis of a chemically cross-linked ferrous-methylthymol blue-polyvinyl alcohol radiochromic gel dosimeter. Applied Radiation and Isotopes 2019, 153:108812.

[45] Gallo S, Artuso E, Brambilla M, Gambarini G, Lenardi L, Monti A F, Torresin A, Pignoli E and Veronese I. Characterization of radiochromic PVA-GTA Fricke gels for dosimetry in X-rays external radiation therapy. Journal of Physics D: Applied Physics 2019, 52(22):225601.

[46] Gallo S, Gambarini G, Veronese I, Argentiere S, Gargano M, Ianni L, Lenardi C, Ludwig N, Pignoli E and d'Errico F. Does the gelation temperature or the sulfuric acid concentration influence the dosimetric properties of radiochromic PVA-GTA Xylenol Orange Fricke gels?. Radiation Physics and Chemistry 2019, 160:35-40.

[47] Lazzeri L, Marini A, Cascone MG, d'Errico F, Dosimetric and chemical characteristics of Fricke gels based on PVA matrices cross-linked with glutaraldehyde. Physics in Medicine and Biology 2019, 64(8): 085015.

[48] SIGMA Product Specification of Mowiol® 18-88 Mw https://www.sigmaaldrich.com/catalog/product/aldrich/81365?lang=it&region=IT (last access at September 2020).

[49] Gallo S, Lizio D, Monti A F, Veronese I, Brambilla M G, Lenardi C, Torresin A, Gambarini G. Temperature behavior of radiochromic poly(vinyl-alcohol)–glutaraldehyde Fricke gel dosimeters in practice. Journal of Physics D: Applied Physics 2020, 53:365003.

[50] Gueli AM, Pasquale S, Politi G, Stella G. The Role of Scale Adjustment in Color Change Evaluation, Instruments 2019, 3:42.

[51] Oleari C. Standard Colorimetry: Definitions, Algorithms and Software. John Wiley & Sons, Wiley Online Library 2016, ISBN: 9781118894477.

[52] Wyszecki G., Stiles W.S. Color science: concepts and methods, quantitative data and formulae. John Wiley and Sons, New York. 1982, ISBN: 978-0-471-39918-6.

[53] Hunt R W G, Pointer M R. Measuring Colour, Wiley Ed. 2011, ISBN: 978-1-119-97537-3.

[54] Liosi G, Dondi D, Vander Griend G, Lazzaroni S. d'Agostino and Mariani M. Fricke-gel dosimeter: overview of Xylenol Orange chemical behavior. Radiation Physics and Chemistry 2017, 140:74-77.

[55] Mokrzycki WS, Tatol M. Colour difference DE: a survey. Mach Graphics Vis. 2011, 20:383–411.

Table 1 – ΔL^*, Δa^*, Δb^*, ΔE^*_{ab} values, calculated using as reference the un-irradiated gel, and the related uncertainties for each irradiation dose (Gy) are listed. The uncertainties have been calculated according to the error propagation theory.

Dose (Gy)	**ΔL***	**Δa***	**Δb***	$\boldsymbol{\Delta E^*_{ab}}$
5	-16.8 ±0.1	5.7 ±0.1	-25.5 ±0.2	31.1 ±0.2
7	-21.6 ±0.1	6.7 ±0.1	-32.7 ±0.2	39.7 ±0.2
10	-29.3 ±0.1	7.9 ±0.1	-46.0 ±0.2	55.1 ±0.2
15	-38.2 ±0.1	8.8 ±0.1	-61.9 ±0.2	73.3 ±0.2
20	-44.5 ±0.2	9.0 ±0.1	-74.3 ±0.2	87.1 ±0.3
25	-48.7 ±0.2	8.7 ±0.1	-83.8 ±0.2	97.3 ±0.2
30	-51.8 ±0.1	8.2 ±0.1	-91.8 ±0.2	105.8 ±0.2

Table 2 – The exponential fit parameters of the L* and b* coordinates obtained by color measurements.

CC	A	B	C	R^2
L*	60.3±0.4	15.1±0.3	11.8±0.5	0.9998
b*	120.9±1.5	20.9±0.5	-19.7±1.6	0.9998

Table 3 – The parameters of linear regressions (m, q and R^2) of the reconstructed dose are listed together with the mean ΔDose for the considered times. All the values are reported with the associated errors (Δm, Δq and σ).

Time (week)	m±Δm	q±Δq	Mean ΔDose± σ	R^2
0	1.003±0.005	0.00±0.05	0.07±0.09	0.9999
1	1.004±0.006	1.15±0.06	1.15±0.07	0.9998
2	1.008±0.005	2.05±0.05	2.11±0.06	0.9998

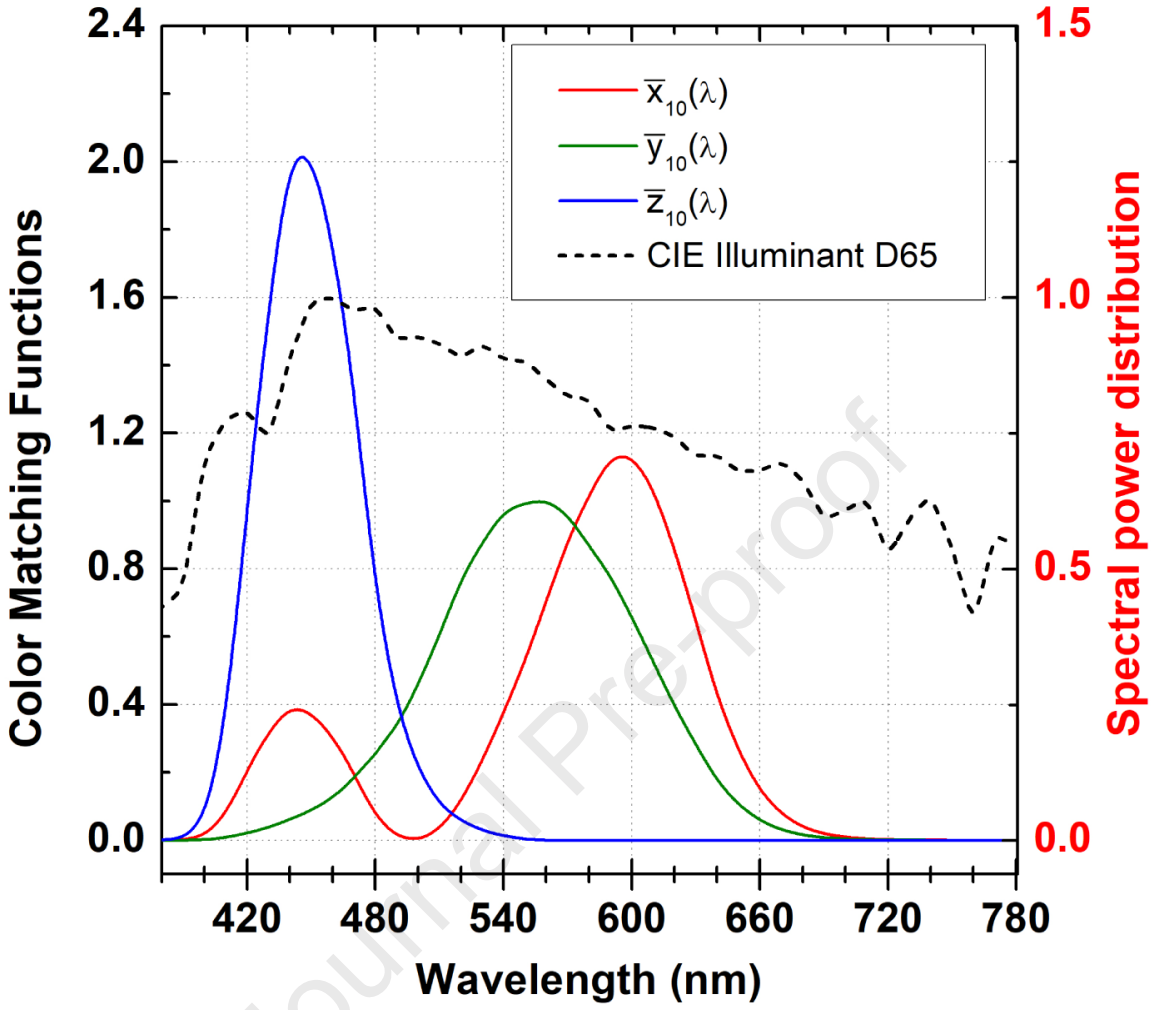

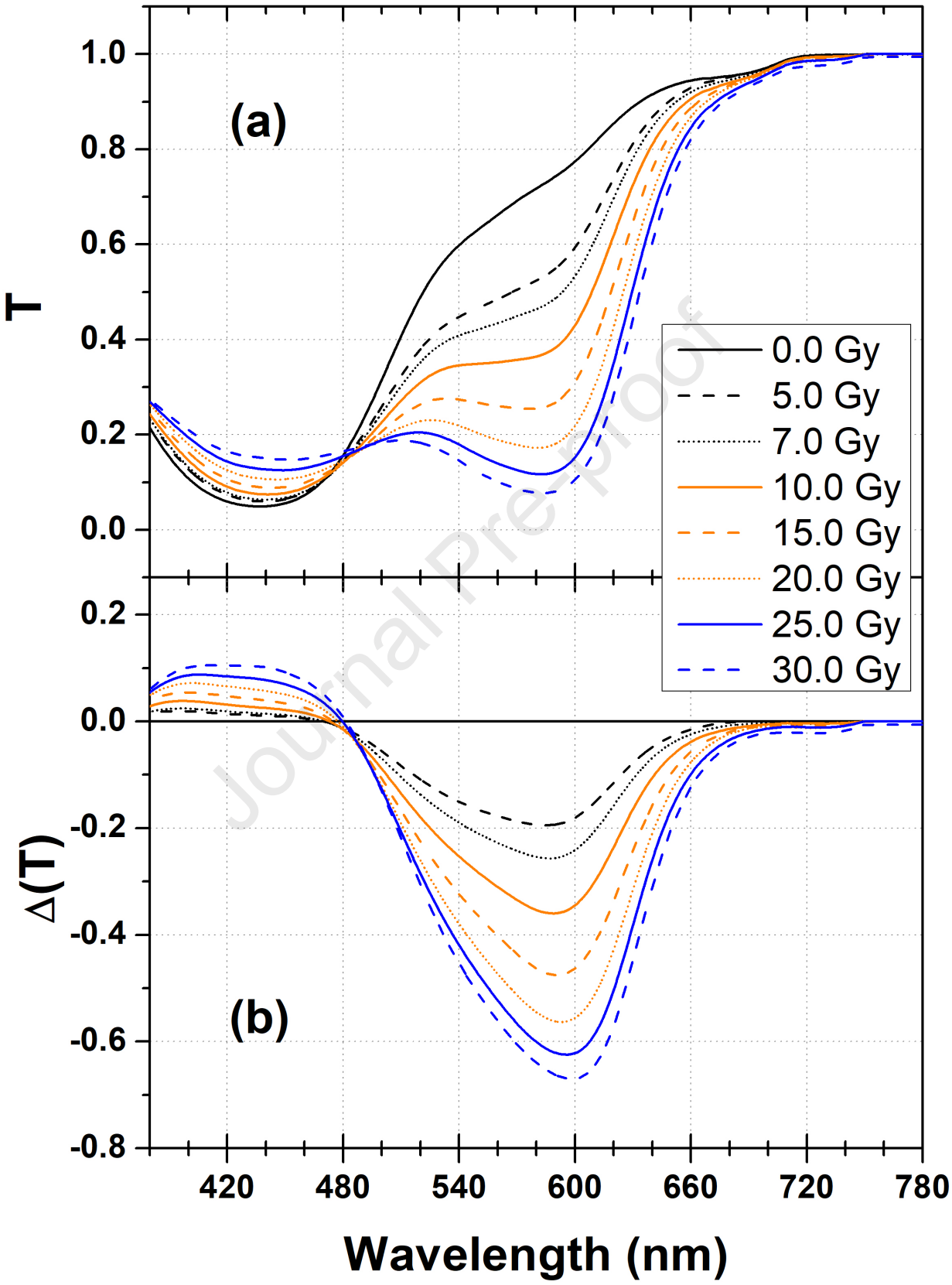

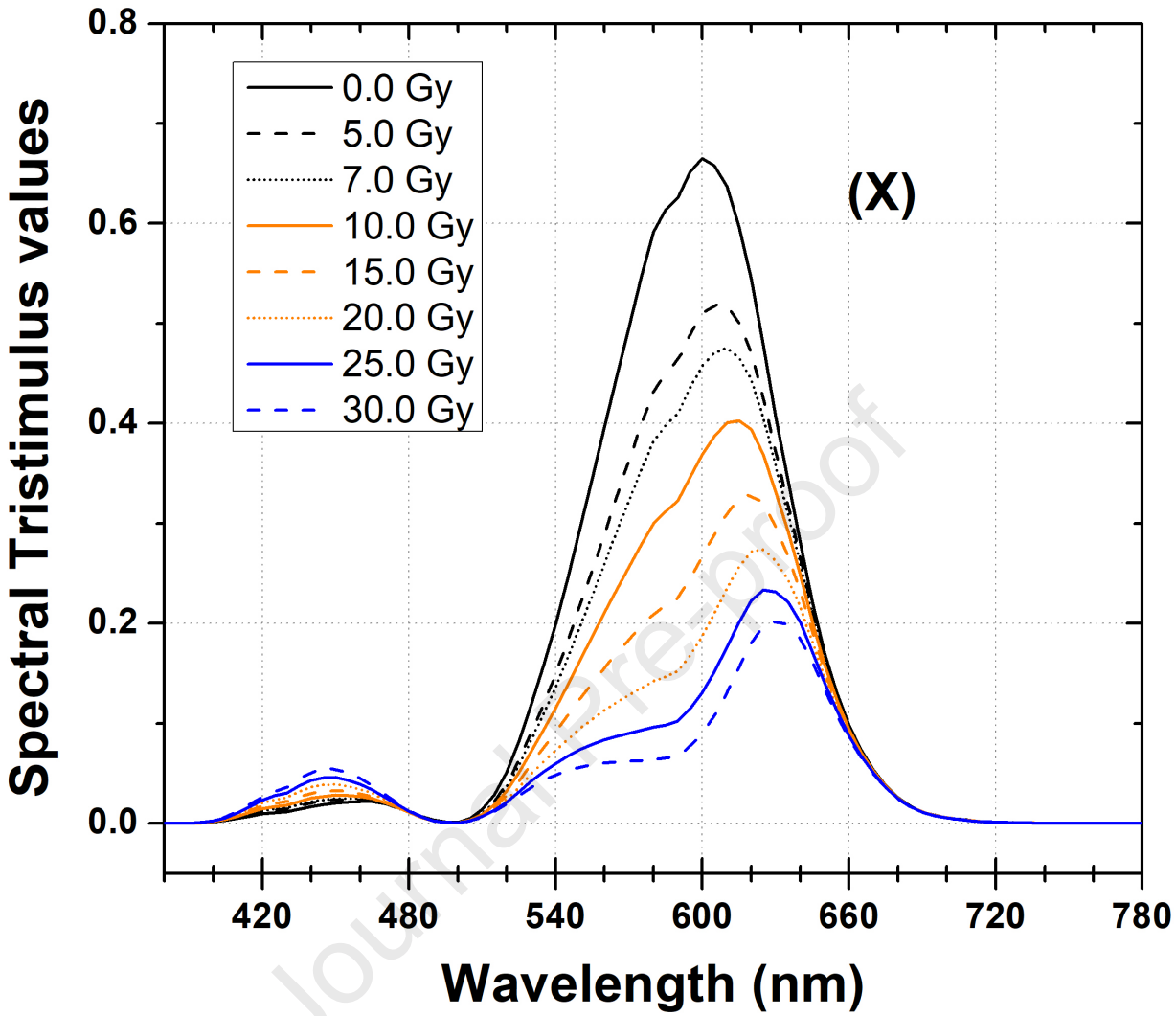

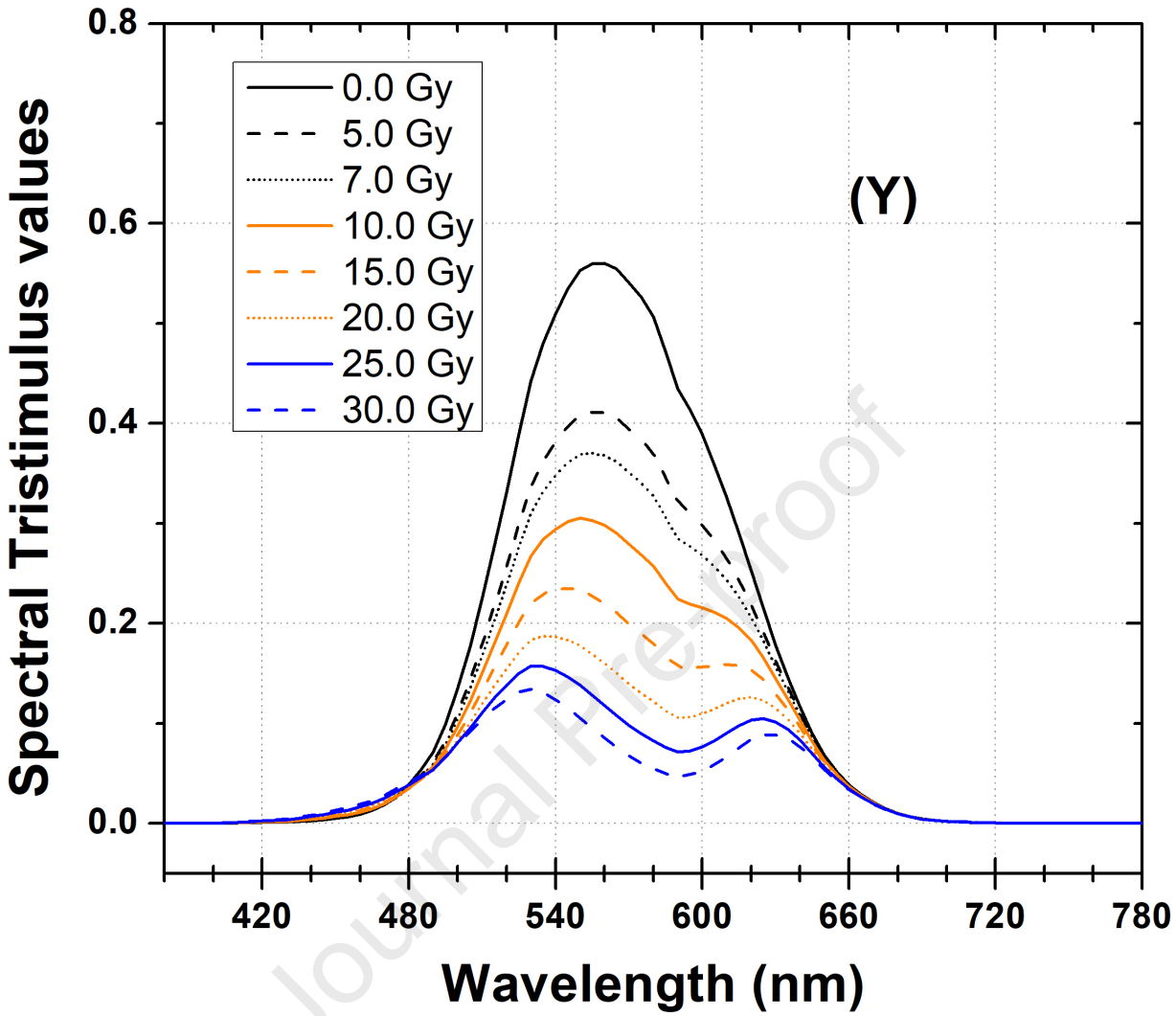

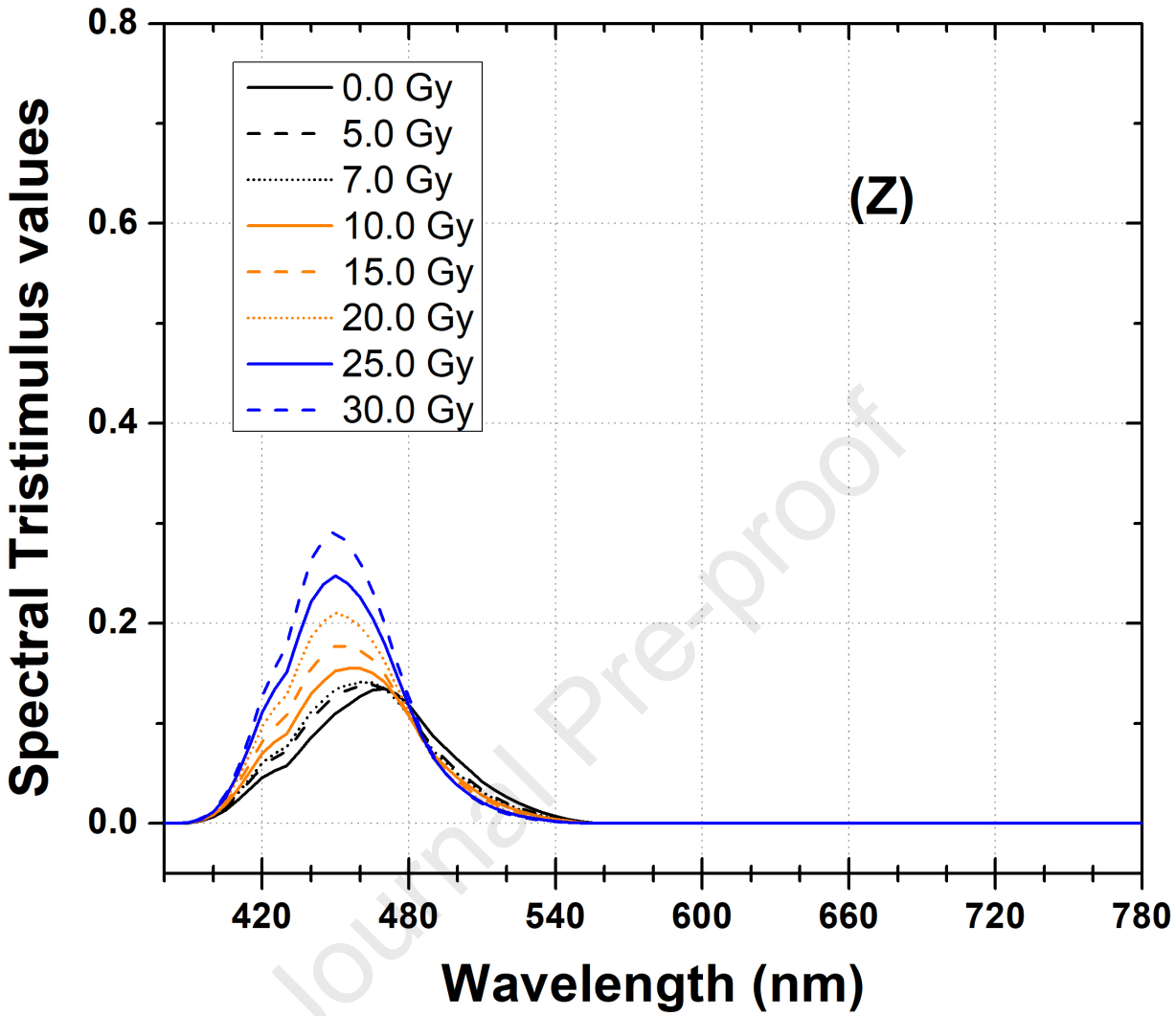

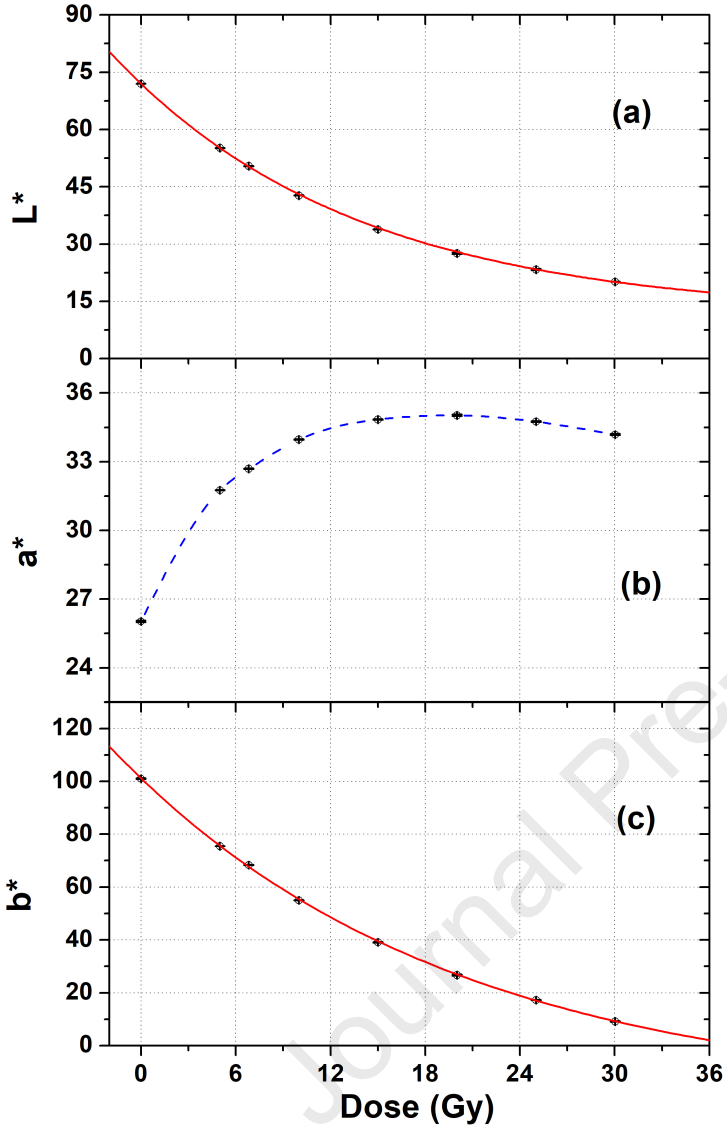

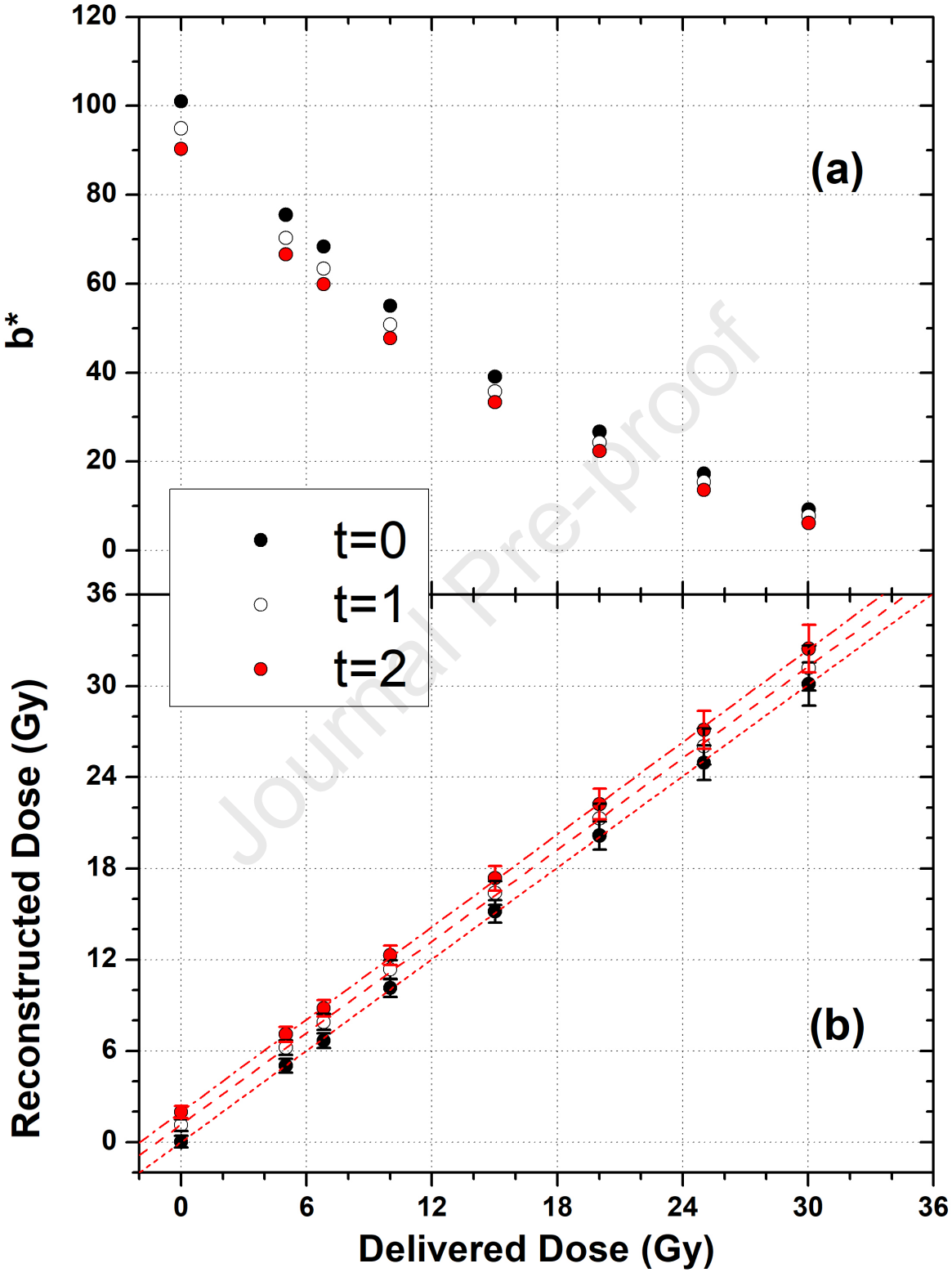

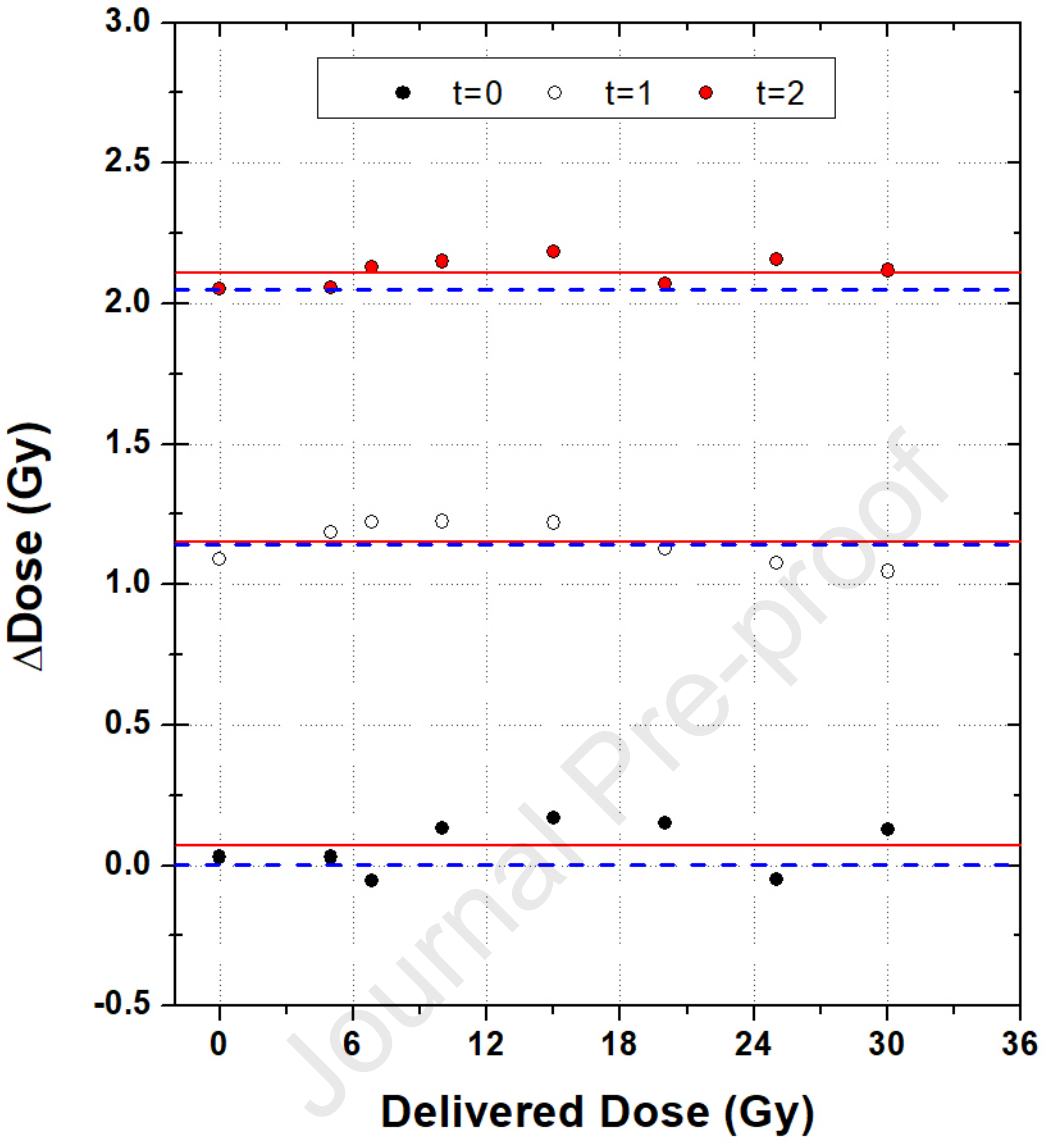

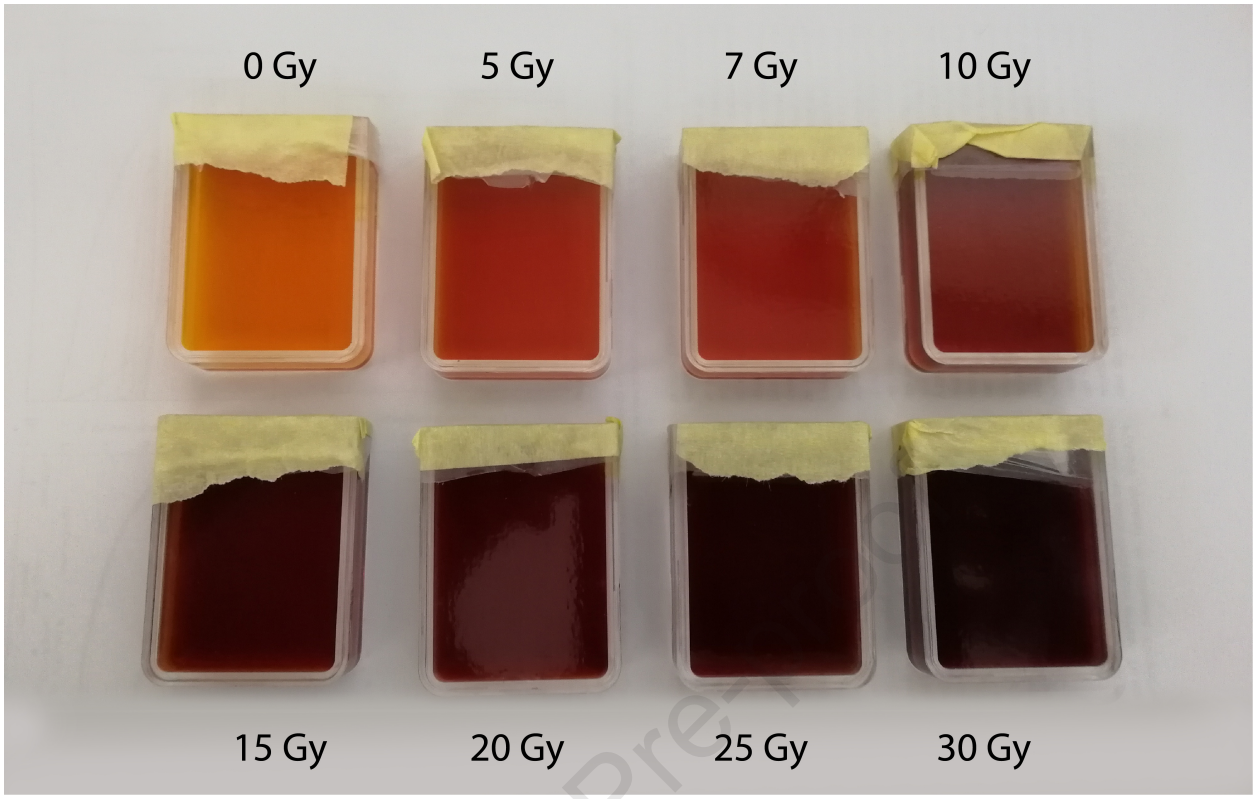

HIGHLIGHTS

- The color specification of the Fricke gels has been performed.
- L* and b* follow a decrescent exponential trend with increasing dose values.
- Reconstructed dose values are calculated at different times in 0-30 Gy.
- Gels, measured at different times, oxide in an equal way with the considered dose-range.

Declaration of interests

Paper title: Effect of ionizing radiation on the colorimetric properties of PVA-GTA Xylenol Orange Fricke gel dosimeters

Authors: Salvatore Gallo, Stefania Pasquale, Cristina Lenardi, Ivan Veronese, Anna Maria Gueli

☒ The authors declare that they have no known competing financial interests or personal relationships that could have appeared to influence the work reported in this paper.

☐The authors declare the following financial interests/personal relationships that may be considered as potential competing interests: